Catalysis Science & Technology

COMMUNICATION

View Article Online
View Journal | View Issue

Cite this: *Catal. Sci. Technol.*, 2018, **8**, 2051

Received 23rd January 2018,
Accepted 8th March 2018

DOI: 10.1039/c8cy00163d

rsc.li/catalysis

Methane activation over a boron nitride catalyst driven by *in situ* formed molecular water†

Yang Wang,[a] Liyang Zhao,[b] Lei Shi,[a] Jian Sheng,[a] Weiping Zhang,[a] Xiao-Ming Cao,*[b] Peijun Hu[b] and An-Hui Lu*[a]

Boron nitride can catalyze the oxidative conversion of methane to valuable chemicals with minor formation of CO_2. B–O–H groups, both originally existing and *in situ* generated in the reaction, promote the activation of O_2 and CH_4, and a novel H_2O-assisted O_2 and CH_4 synergetic mutual activation mechanism was proposed.

Hexagonal boron nitride (h-BN) is an emerging and revolutionary metal-free catalyst for the oxidative dehydrogenation of ethane,[1] propane[2] and butane,[3] exhibiting higher olefin selectivity with only negligible CO_2 formation compared to traditional metal-based catalysts. Actually, as a graphite-like material, h-BN with excellent structural and thermal stability[4] has been widely accepted as a catalytically inert material for a quite long time.[5] Thus, the activity origin of h-BN in the catalytic dehydrogenation of alkanes has aroused widespread interest. Hermans's group proposed that oxygen-terminated armchair h-BN edges act as the catalytically active sites, and dehydrogenation occurs *via* the abstraction of a hydrogen atom from the secondary carbon of propane by breaking the O–O bond of >B–O–O–N<,[2b] afterwards, they rediscovered the mechanism whereby surface-stabilized BOx sites formed under the reaction conditions act as active sites.[6] Su's group put forward a different mechanism in the dehydrogenation of ethane and they thought that the presence of ethane promoted the activation of adsorbed O_2 on the edges of h-BN to form B–O(H) sites, which then abstracted hydrogen from ethane to ethene.[1b] In our previous work, we demonstrated that B–OH groups were generated after steam treatment of h-BN, and then the hydrogen abstraction of B–O–H by molecular oxygen dynamically generated the B–O$^{\bullet}$ sites, which triggered propane dehydrogenation by playing the role of active sites.[2a] Although there is a fairly clear consensus that h-BN can selectively break the C–H bond and inhibits over-oxidation of C_2–C_4 alkanes under an oxidative atmosphere, further study is needed to explore whether h-BN can activate more stable methane molecules and to understand the activation mechanism in-depth.

Methane, as the main component of natural gas, shale gas and gas hydrate resources, is an important feedstock for the production of value-added chemicals and fuels.[7] However, the activation and conversion of methane are much more difficult and remain a great challenge due to its stable tetrahedral structure, high bond energy (434 kJ mol^{-1})[8] and low polarizability (2.84×10^{-40} C^2 m^2 J^{-1}).[9] To date, the oxidative conversion of methane is mainly carried out over metal[10] or metal oxide[11] catalysts. The investigation of the catalytic ability of h-BN towards the activation and conversion of methane will not only result in an improved catalyst system, but also enhance our fundamental understanding in terms of the oxidative dehydrogenation ability of h-BN at the molecular level.

In this work, we demonstrated a h-BN catalyst being able to catalyze the oxidative conversion of methane and put

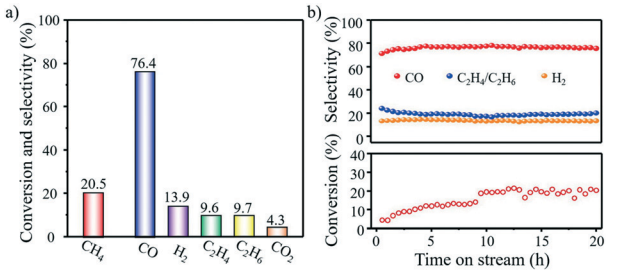

Fig. 1 Selective oxidation of methane over the h-BN catalyst: a) influence of temperature on catalytic activity and selectivity, b) long-term stability test at 690 °C. Reaction conditions: catalyst, 100 mg; gas feed, 28.6 vol% CH_4, 14.3 vol% O_2, N_2 balance; gaseous hourly space velocity 21 000 mL g_{cat}^{-1} h^{-1}.

[a] *State Key Laboratory of Fine Chemicals, School of Chemical Engineering, Dalian University of Technology, Dalian 116024, P. R. China.*
E-mail: anhuilu@dlut.edu.cn
[b] *Centre for Computational Chemistry and Research Institute of Industrial Catalysis, School of Chemistry and Molecular Engineering, East China University of Science and Technology, Shanghai 200237, P. R. China.*
E-mail: xmcao@ecust.edu.cn

† Electronic supplementary information (ESI) available. See DOI: 10.1039/c8cy00163d

forward a novel methane activation mechanism based on the experimental and theoretical studies. The commercial h-BN was purified with NH_3H_2O and calcined in air before use. The selective oxidation of methane was performed in a packed-bed quartz microreactor under atmospheric pressure using a feed gas containing methane, oxygen and nitrogen (2 : 1 : 4). The conversion of methane is stabilized at 20.5% at 690 °C (Fig. 1a). The products include CO (76%), H_2 (14%), C_2H_4 (10%), C_2H_6 (10%), and CO_2 (4%). By raising the temperature to 720 °C, the methane conversion nearly doubled to 37.0%, while the selectivity for CO and H_2 increased slightly to 81.4% and 17.8%, respectively, and the selectivity for C_2H_4 and C_2H_6 decreased to 6.7% and 3.8%, respectively (Fig. S1†). The stability of the h-BN catalyst was tested at a constant temperature of 690 °C for 20 h. The CH_4 conversion gradually increased during the first 10 h to ~20% and then remained stable over the entire test (Fig. 1b). No coke was detected on the catalyst after the 20 h test (Fig. S2†). By comparison, a blank experiment (a reactor with quartz sand) under the same conditions showed a CH_4 conversion of only 5.3% at 720 °C (Fig. S3†).

The origin of the catalytic performance of h-BN in CH_4 conversion was investigated first by structural analysis for fresh and spent catalysts. The surface area of fresh h-BN is 53 m^2 g^{-1} measured by nitrogen physisorption (Fig. S4†). TEM images show a large number of edge sites. The morphology and lattice fringe are unchanged after reaction (Fig. 2a, S5†). The XRD patterns of the fresh catalyst correspond to the lattice planes of hexagonal boron nitride (JCPDS 01-073-2095). After reaction, the catalyst retains the typical hexagonal layered structure (Fig. 2b, S6†).

XPS analysis identified two types of boron species (Fig. 2c, S7†), corresponding to boron associated with nitrogen (B–N) and oxygen (B–O),[12] respectively. Moreover, the proportion of B–O (B–O/(B–N + B–O)) increased rapidly from 0.03 in the fresh catalyst to 0.08 after 2 h and 0.13 after 9 h in the reactor (Fig. 2d), then, the proportion reached a constant value. This change is mainly attributed to the oxidation of h-BN which causes partial substitution of N by O in the h-BN lattice during the reaction.[13] Combined with the stability test result that the conversion of CH_4 gradually increased in the first 9 hours and then remained stable (Fig. 1b), we speculated that the B–O species is related to the catalytic performance.

In our previous work, we demonstrated that both B–O–B and B–O–H sites originally existed in the fresh h-BN catalyst.[2a] To further identify which site or if both are involved in the reaction process, we first studied whether the activation of CH_4 and O_2 can be realized on the B–O–B sites by density functional theory (DFT) calculations. As displayed in Fig. S8a,† if O_2 chemisorbs on the oxidized h-BN with the B–O–B terminal (Fig. S9†), its optimal adsorption energy is −2.12 eV. Such a significantly negative value of adsorption energy indicates that B–O–B could not fix O_2. Furthermore, the first C–H bond dissociation of CH_4 has to overcome the energy barrier as high as 2.29 eV, and the reaction energy of this step is evidently endothermic (Fig. S8b†). Hence, it is formidable for the B–O–B sites to activate either CH_4 or O_2 even at ~700 °C.

We further tracked the dynamic evolution of B–O–H groups under the reaction conditions using IR spectroscopy. When exposed to a helium atmosphere, the position and intensity of the hydroxyl stretches (~3400 cm^{-1}) are unchanged (Fig. S10a†).[14] Similarly, upon exposure to a CH_4 or O_2 atmosphere, the band of the hydroxyl stretches also remains unchanged (Fig. S10b and c†). Nevertheless, when the feed gas was switched to a mixture of CH_4 and O_2, the

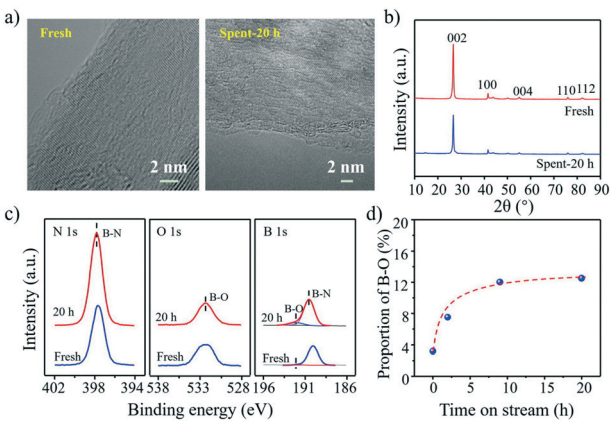

Fig. 2 a) TEM images, b) XRD patterns, c) N 1s, O 1s and B 1s XPS spectra of the fresh and spent catalysts after a 20 h test, d) influence of reaction time on the B–O proportion in B 1s XPS (B–O/(B–O + B–N)).

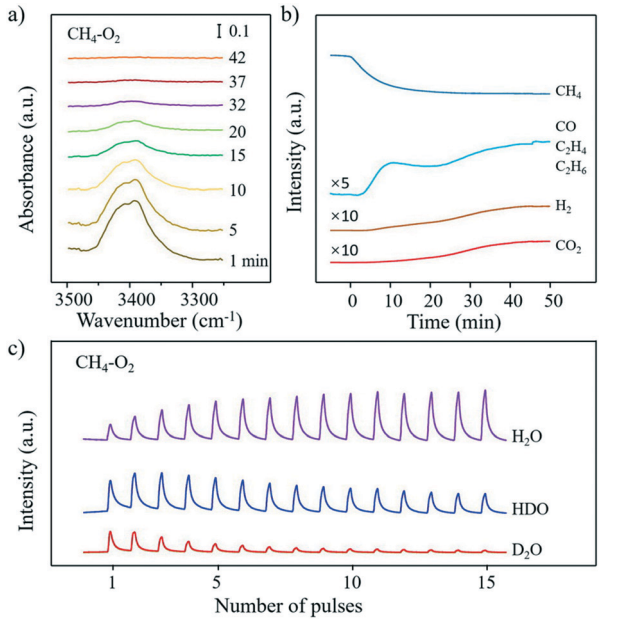

Fig. 3 a) FT-IR spectra of B–OH vibration over the h-BN catalyst under CH_4–O_2 atmospheres, b) mass spectra of CH_4, CO, C_2H_6, C_2H_4, CO_2 and H_2 species, c) mass spectra of H_2O, HDO and D_2O species upon pulsing a mixture of CH_4 and O_2 on the deuterated h-BN catalyst.

intensity of the hydroxyl vibrational stretches gradually weakened (Fig. 3a).

To understand the correlation of the B–O–H with CH_4 activation process, we performed mass spectrometry to detect the products from the IR cell (Fig. 3b). After pulsing the mixture of CH_4 and O_2, as the absorption of the hydroxyl vibrational stretches gradually weakened, the signal intensity of CH_4 detected by MS gradually decreased, whereas the signal of H_2, CO, C_2H_4, and C_2H_6 gradually increased, demonstrating the increased conversion rate of CH_4 over the h-BN catalyst. Subsequently, when the hydroxyl vibrational stretches nearly remain unchanged, the signal intensity of CH_4, H_2, CO, C_2H_4, and C_2H_6 tends to reach a constant value. These results suggest that the B–O–H groups are correlated with the CH_4 activation assisted by oxygen.

Isotope-labelling experiments were carried out to further investigate the role of the B–O–H groups in the methane activation process. Before the test, the fresh h-BN catalyst was treated using heavy water (D_2O) at 590 °C. Solid-state ^1H NMR spectra revealed that the amount of B–OH decreased after this treatment, indicating that some of the –OH groups on the catalyst were replaced by –OD (Fig. S11†). When pulsing a mixture of CH_4 and O_2 into the reaction chamber, HDO and D_2O were generated immediately, in addition to H_2O. In subsequent pulses, the intensity of HDO and D_2O gradually decreased while that of H_2O increased (Fig. 3c). In contrast, when pulsing a mixture of N_2 and H_2O, the intensity of HDO, D_2O and H_2O almost remained unchanged (Fig. S12a†), and the same result was obtained when pulsing a mixture of CH_4 and H_2O (Fig. S12b†) or a mixture of O_2 and H_2O (Fig. S12c†). These results clearly indicate that the H/D atoms in the h-BN catalyst are abstracted during the CH_4 conversion process rather than just re-exchanged by H_2O *in situ* generated in the reaction. It also shows that a dynamic exchange between the H atoms in the –OH groups of the catalyst surface and CH_4 molecule occurs during the reaction. In contrast, when only O_2 was pulsed in, no water isotopologs were detected (Fig. S13a†), suggesting that molecular O_2 cannot be activated by the surface –OH (D) groups. Similarly, no products appeared when only CH_4 was pulsed in (Fig. S13b†), indicating that surface –OH groups are incapable of activating CH_4 in the absence of O_2.

To further elucidate the reaction mechanism, we studied the possible reaction pathways by DFT calculations. Although it is difficult for B–O–B to activate either CH_4 or O_2, B–O–B could readily be converted to B–O–H in the presence of water (Fig. S14a†), which only needs to overcome an energy barrier of 0.67 eV for the transformation. This exothermic process releases an energy of 0.25 eV, implying a favorable transformation from B–O–B to B–O–H in the presence of water. This result is consistent with our previous work.[2a] Interestingly, with the formation of B–O–H, albeit still thermodynamically unfavorable, the adsorption strength of O_2 could remarkably be improved from −2.12 eV on B–O–B to −0.66 eV on B–O–H (Fig. S8a†), indicating the probability of forming transient intermediate O_2* (the asterisk denotes the surface species) on B–O–H. O_2 could achieve more than 1 e from BN with B–O–H (BNOH) and the O–O bond is stretched to 1.522 Å if it is chemisorbed. However, as indicated in Fig. S8b,† it is still rather drastic for BNOH to directly activate CH_4. The first C–H bond dissociation on BNOH has to conquer an extremely high energy barrier of 2.52 eV, which is even higher than that on B–O–B.

More interestingly, the adsorbed O_2 on BNOH could significantly facilitate the activation of CH_4. The energy barrier of the first C–H bond dissociation is dramatically reduced to 0.90 eV. After the C–H bond scission process (Fig. S14b†), the O–O bond could also be broken. Taking the effect of water for the formation of BNOH on the enhanced O–O activation into account, this sheds light on a novel H_2O-assisted O_2 and CH_4 synergetic mutual activation mechanism. This may be attributed to the fact that the formation of BNOH partially weakens the neighboring B–N bond strength, which makes it possible to promote the O_2 activation to some extent. This leads to the formation of transient surface active peroxide species which could possibly activate CH_4. Moreover, during the C–H bond oxidative dissociation, the obtained electrons from CH_4 could further activate the O–O bond, resulting in its scission (Fig. S14b†). This synergetic mechanism can explain the reason why no reaction occurs under either an independent CH_4 or O_2 flow, and also no chemisorbed species could be found after either an independent CH_4 or O_2 flow on BNOH (Fig. S15 and S16†).

The CH_4 and O_2 activation triggers the subsequent surface and gaseous radical reactions towards the formation of C_2H_6, CO, H_2 and H_2O. As depicted in Fig. 4a, at 690 °C, the

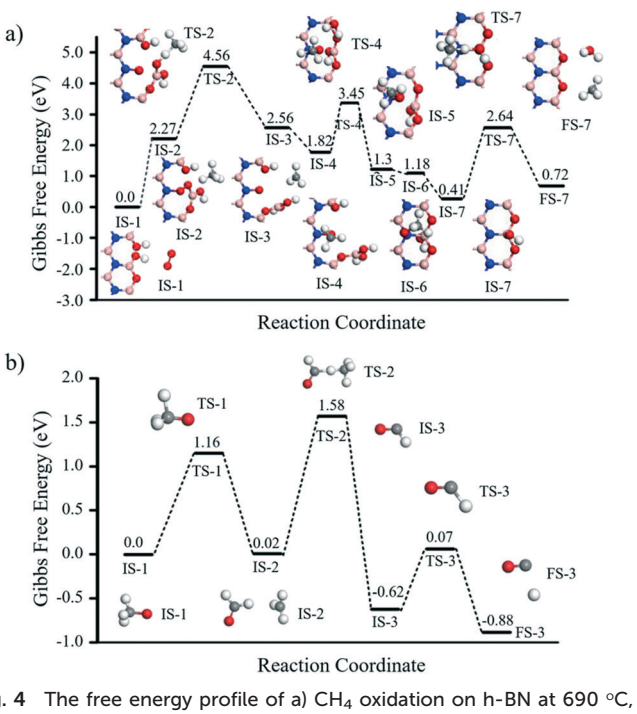

Fig. 4 The free energy profile of a) CH_4 oxidation on h-BN at 690 °C, and the corresponding b) gaseous radical reactions towards CO formation at 690 °C.

produced gaseous $CH_3^{\bullet}$ free radical (IS-3) could preferentially bind to the O terminal of the formed N=O bond at a low flow rate to form OCH3* (IS-4) whose Gibbs free energy goes downhill by 0.74 eV. After the recovery of the B–O–B edge *via* hydrogen transfer and water desorption (IS-5), the broken B–N bond during O_2 chemisorption could be readily re-formed (IS-6). Consequently, the weakening of the N–CH_3O bond due to the formation of the B–N bond makes CH_3O* possible to be desorbed to form a gaseous free radical, even releasing 0.77 eV at 690 °C (IS-7). Then the remaining OH* vertically adsorbed at the B site could readily activate CH_4 with a free energy barrier of 2.23 eV, followed by the recovery of BN from B–O–B.

During the above surface reaction cycling, two free radical species, $CH_3^{\bullet}$ and $CH_3O^{\bullet}$, are likely to be produced at one site, especially under the condition of a low flow rate. C_2H_6 could be readily obtained *via* the homocoupling of $CH_3^{\bullet}$ in the gas phase, releasing an energy of 2.06 eV (Table S1†). $CH_3O^{\bullet}$ is easily dissociated to stable closed-shell HCHO and $H^{\bullet}$ in the gas phase. Two possible deep dehydrogenation branch pathways could start with HCHO towards the formation of CO: (I) reacting with the active surface oxygen species; (II) reacting with free radical $CH_3^{\bullet}$. For pathway I, $HCHO^{\bullet}$ could readily be dehydrogenated by the O_2* adsorbed on h-BN or surface intermediate OH*–B (IS-7), respectively, with free energy barriers of 1.43 eV and 1.57 eV (at 690 °C). It is also very likely for the H of HCHO to be abstracted by $CH_3^{\bullet}$ to yield $CHO^{\bullet}$ at reaction pathway II, climbing uphill a free energy barrier of 1.56 eV (Fig. 4b). The similar free energy barriers indicate that once HCHO is produced, it would be subjected to deep oxidation either catalyzed by h-BN or *via* a gas radical reaction. The formed $CHO^{\bullet}$ radical is easily decomposed to CO and $H^{\bullet}$. Hence, CO is formed from the deep dehydrogenation of $CH_3O^{\bullet}$. Moreover, H_2 is formed *via* the homocoupling of $H^{\bullet}$ from the direct decomposition of the open-shell $CH_3O^{\bullet}$ and $CHO^{\bullet}$ radical. Yet due to the presence of O_2, the H of $CHO^{\bullet}$ is also likely to be abstracted from O_2 towards the final product H_2O (Table S1†). Since the initial formation of $CH_3O^{\bullet}$ depends on the $CH_3^{\bullet}$ re-adsorption on h-BN, more CO is yielded due to the higher collision possibility between $CH_3^{\bullet}$ and h-BN under the condition of a low flow rate while more C_2H_6 is produced under the condition of a high flow rate (Fig. S17†).

Conclusions

In conclusion, we have demonstrated that boron nitride can catalyze the oxidative conversion of methane to valuable chemicals, with minor formation of CO_2. Our experimental and theoretical studies reveal that the hydroxylated h-BN can adsorb O_2, and then the activation of adsorbed O_2 and gaseous CH_4 occurs through a synergetic mutual activation mechanism. The CH_4 and O_2 activation triggers subsequent surface and gaseous radical reactions towards the formation of C_2H_6, C_2H_4, CO, H_2, CO_2 and H_2O. This metal-free h-BN catalyst enriches our knowledge of methane activation and might lead to new possibilities for the development of more sustainable methane conversion schemes.

Conflicts of interest

There are no conflicts to declare.

Acknowledgements

This study was supported by the State Key Program of the National Natural Science Foundation of China (21733002 and 21333003) and the National Natural Science Foundation of China (U1462120 and 21673072).

Notes and references

1 (*a*) L. Shi, B. Yan, D. Shao, F. Jiang, D. Q. Wang and A. H. Lu, *Chin. J. Catal.*, 2017, **38**, 389–395; (*b*) R. Huang, B. S. Zhang, J. Wang, K. H. Wu, W. Shi, Y. J. Zhang, Y. F. Liu, A. M. Zheng, R. Schlögl and D. S. Su, *ChemCatChem*, 2017, **9**, 3293–3297.

2 (*a*) L. Shi, D. Q. Wang, W. Song, D. Shao, W. P. Zhang and A. H. Lu, *ChemCatChem*, 2017, **9**, 1788–1793; (*b*) J. T. Grant, C. A. Carrero, F. Goeltl, J. Venegas, P. Mueller, S. P. Burt, S. E. Specht, W. P. McDermott, A. Chieregato and I. Hermans, *Science*, 2016, **354**, 1570–1573.

3 J. M. Venegas, J. T. Grant, W. P. McDermott, S. P. Burt, J. Micka, C. A. Carrero and I. Hermans, *ChemCatChem*, 2017, **9**, 2118–2127.

4 J. Yin, J. D. Li, Y. Hang, J. Yu, G. A. Tai, X. M. Li, Z. H. Zhang and W. L. Guo, *Small*, 2016, **22**, 2942–2968.

5 (*a*) Q. H. Weng, X. B. Wang, X. Wang, Y. Bandoa and D. Golberg, *Chem. Soc. Rev.*, 2016, **45**, 3989–4012; (*b*) A. Pakdel, Y. Bando and D. Golberg, *Chem. Soc. Rev.*, 2014, **43**, 934–959.

6 J. T. Grant, W. P. McDermott, J. M. Venegas, S. P. Burt, J. Micka, S. P. Phivilay, C. A. Carrero and I. Hermans, *ChemCatChem*, 2017, **9**, 3623–3626.

7 (*a*) B. W. Wang, S. Albarracín-Suazo, Y. Pagán-Torres and E. Nikolla, *Catal. Today*, 2017, **285**, 147–158; (*b*) P. Tang, Q. J. Zhu, Z. X. Wu and D. Ma, *Energy Environ. Sci.*, 2014, **7**, 2580–2591; (*c*) D. A. Hickman and L. D. Schmidt, *Science*, 1993, **259**, 343–346; (*d*) K. Narsimhan, V. K. Michaelis, G. Mathies, W. R. Gunther, R. G. Griffin and Y. Roman-Leshkov, *J. Am. Chem. Soc.*, 2015, **137**, 1825–1832.

8 X. G. Guo, G. Z. Fang, G. Li, H. Ma, H. J. Fan, L. Yu, C. Ma, X. Wu, D. H. Deng, M. M. Wei, D. L. Tan, R. Si, S. Zhang, J. Q. Li, L. T. Sun, Z. C. Tang, X. L. Pan and X. H. Bao, *Science*, 2016, **344**, 616–619.

9 P. Schwach, X. L. Pan and X. H. Bao, *Chem. Rev.*, 2017, **117**, 8497–8520.

10 (*a*) D. A. Hickman and L. D. Schmidt, *Science*, 1993, **259**, 343–346; (*b*) T. V. Choudhary and V. R. Choudhary, *Angew. Chem., Int. Ed.*, 2008, **47**, 1828–1847; (*c*) B. C. Enger, R. Lødeng and A. Holmen, *Appl. Catal., A*, 2008, **346**, 1–27; (*d*) C. Okolie, Y. F. Belhseine, Y. Lyu, M. M. Yung, M. H.

Engelhard, L. Kovarik, E. Stavitski and C. Sievers, *Angew. Chem., Int. Ed.*, 2017, **56**, 13876–13881.

11 (*a*) G. J. Hutchings, *Chem. Soc. Rev.*, 1989, **18**, 251–283; (*b*) J. H. Lunsford, *Angew. Chem., Int. Ed. Engl.*, 1995, **34**, 970–980; (*c*) K. Kwapien, J. Paier, J. Sauer, M. Geske, U. Zavyalova, R. Horn, P. Schwach, A. Trunschke and R. Schlögl, *Angew. Chem., Int. Ed.*, 2014, **53**, 8774–8778.

12 K. H. Lee, H. J. Shin, B. Kumar, H. S. Kim, J. Lee, R. Bhatia, S. H. Kim, I. Y. Lee, H. S. Lee, G. H. Kim, J. B. Yoo, J. Y. Choi and S. W. Kim, *Angew. Chem., Int. Ed.*, 2014, **53**, 11493–11497.

13 K. A. Simonov, N. A. Vinogradov, M. L. Ng, A. S. Vinogradov, N. Mårtensson and A. B. Reobrajenski, *Surf. Sci.*, 2012, **606**, 564–570.

14 (*a*) A. Bhattacharya, S. Bhattacharya and G. P. Das, *Phys. Rev. B: Condens. Matter*, 2012, **85**, 035415; (*b*) T. Sainsbury, A. Satti, P. May, Z. Wang, I. McGovern, Y. K. Gun'ko and J. Coleman, *J. Am. Chem. Soc.*, 2012, **134**, 18758–18771.